ELSEVIER

Colloids and Surfaces
A: Physicochemical and Engineering Aspects 177 (2001) 99–110

COLLOIDS AND SURFACES A

www.elsevier.nl/locate/colsurfa

A micromechanics approach for attachment and detachment of asymmetric colloidal particles

Talat Mahmood *, Appiah Amirtharajah, Terry W. Sturm, Keith E. Dennett [1]

School of Civil and Environmental Engineering, Georgia Institute of Technology, Atlanta, GA 30332, USA

Abstract

In this study, a micromechanics interaction model has been developed for kaolinite particles, and experiments have been performed on attachment and detachment of particles in porous media columns. The experimental results are discussed and interpreted in terms of microscopic forces, in contrast to conventional computations in the colloid literature which are based on energy terms. The force calculations are done using expressions developed for the natural shape (hexagonal platelets) of the kaolinite particles without making use of unrealistic assumptions of particle sphericity. The forces considered are van der Waals forces, electrical double layer forces, hydration forces and Born repulsion. Under constant chemical conditions, the three likely modes of interaction of kaolinite platelets showed significantly different total force curves. The microscopic force analysis was found to be consistent with experimental results. © 2001 Elsevier Science B.V. All rights reserved.

Keywords: Micromechanics; Laolinite; Colloidal particles

1. Introduction

Particle detachment is a physico-chemical process, which occurs when hydrodynamic forces or physico-chemical forces or both overcome adhesive interparticle forces. A mechanistic understanding of the detachment phenomenon has implications in various fields of environmental engineering such as floc break up in solid–liquid separation processes, colloid-facilitated transport of contaminants, in current theories of deep-bed filtration, and in backwashing of filters. Unfortunately, analysis of interaction of asymmetric colloidal particles has received inadequate attention in the past despite the fact that most of the naturally occurring particles are asymmetric. The focus of this research is on the development and experimental validation of theoretical formulae, which could be used to better analyze the interactions between naturally occurring asymmetric particles without making use of oversimplifying assumptions of particle sphericity.

Colloid scientists have generally analyzed particle interactions using energies of interaction rather than forces experienced by the particles because it is easier to deal with the potential

* Corresponding author. Present address: PAPRICAN, 570 St. Jean Blvd., Pointe Claire, Quebec, Canada H9R 3J9. Tel.: + 1-514-6304100; fax: + 1-514-6304134.

E-mail address: tmahmood@paprican.ca (T. Mahmood).

[1] Present address: Department of Civil Engineering, University of Nevada, Reno, Nevada 89557-0152, USA

0927-7757/01/$ - see front matter © 2001 Elsevier Science B.V. All rights reserved.
PII: S0927-7757(00)00663-4

energy of interaction between particles than the interparticle forces [1]. However, it is the forces between the macroscopic bodies that are often easier to measure, and of greater interest, rather than their interaction energies [2]. [3] showed that force and energy calculations provided different results for the DLVO model at short distances of separation (below 10 nm); and the force calculations provided a better understanding of the particle attachment and detachment phenomena. Therefore, in order to develop a satisfactory model for particle detachment, the interparticle interactions have to be quantified in terms of forces instead of conventional energy terms [3]. [3] analyzed detachment of spherical particles from flat surfaces and large spheres. Analysis in force terms will allow synthesis of macroscopic forces (DLVO and non-DLVO forces) to make comparisons with macroscopic parameters such as hydrodynamic forces.

Kaolinite particles exist in nature as thin hexagonal platelets having two large flat faces and approximately rounded edges. The electrochemical properties of a face are markedly different from those of an edge. The cleavage planes (faces) of the platelets are negatively charged while the edges are positively charged under acidic conditions and the edge charge is pH dependent. With a hexagonal platelet representation, kaolinite platelets may associate in three possible modes of interaction; namely, face–face (F–F), edge–face (E–F), edge–edge (E–E). [4] developed an energy interaction model for kaolinite particles wherein the face surface was represented by a flat plate and the edges as a sphere. However, there exists microscopic evidence [5] that edges of the kaolinite platelets are not flat but rounded like a half cylinder. [6] criticized the approach of [4] and used DLVO theory alone to formulate an energy interaction model for kaolinite particles in which the platelet edges were represented by cylinders rather than spheres. The DLVO theory-based energy models of both [4,6] fail to obtain primary minima of finite depths, and incorrectly predict infinite attraction energy as the separation distance approaches zero at all ionic strength and pH values, which necessitates an assumption of equilibrium separation distance. The absence of finite primary minima prevents these models from being used to compare net adhesive forces under varied solution compositions. In particular, these models become extremely unreliable in predicting particle detachment since the attached particles are located at the primary minima, prior to detachment. The theory presented in this paper provides a rational approach to this problem by combining hydration forces and Born repulsion with DLVO forces. It determines the location and makes the depths of the primary minima finite, and therefore allows computation of net adhesive forces under various solution chemistries.

2. Theoretical developments

A representative kaolinite platelet with two hexagonal flat faces and rounded edges is shown in Fig. 1. Because of the electrokinetic properties of kaolinite platelets, three modes of interparticle interaction, F–F, E–F, and E–E, are possible depending upon the physico-chemical environment. In this research, expressions have been developed for electrical double layer forces, hydration forces, and Born repulsion for the three likely modes of interaction of these asymmetric particles.

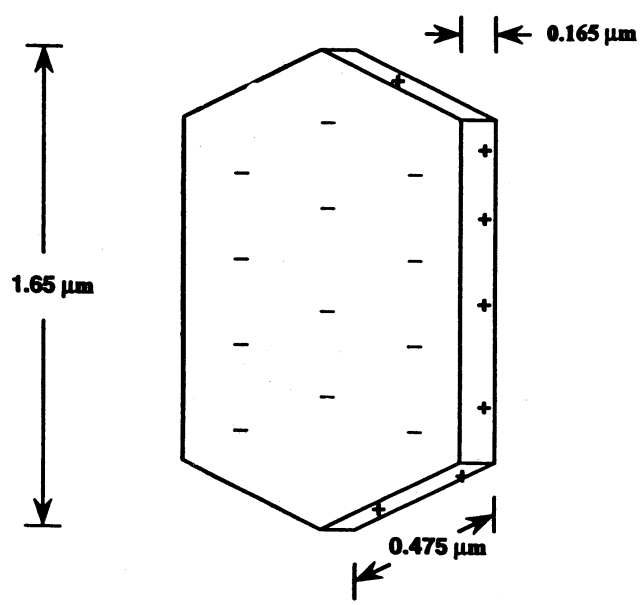

Fig. 1. A representative kaolinite platelet.

In most natural systems coarse particles are covered with layers of small deposited particles. The detachment process does not release all of the attached particles on surfaces [7]. Therefore, in the development of a realistic conceptual model for particle detachment, it is necessary to analyze the interaction between a single particle and a larger grain coated with a deposited layer of particles [3]. In the following theoretical treatment, the surface of the grains (glass beads) is assumed to be masked by the attached kaolinite platelets, and therefore, only kaolinite–kaolinite interactions are considered during detachment. In the force calculations to follow, it has been assumed that (1) the cleavage surfaces of the kaolinite platelets are flat and they can be represented by flat plates; (2) platelet edges are rounded and their interaction is represented by half cylinders of radii equal to half the thickness of the platelet; (3) the F–F interaction is represented by the flat plate–flat plate interaction; (4) the E–F interaction is represented by the interaction between a flat plate and a half cylinder parallel to it; and (5) the E–E interaction is modeled as the interaction between two similar parallel half cylinders. Similar assumptions were made by [6] in their developments using DLVO theory.

2.1. Hydration force

2.1.1. Face–face hydration force

[8] reported the structural component of the interaction energy per unit area between two parallel plates at a distance z apart to be given by

$$E_{\mathrm{H}} = Kh \exp\left(\frac{-z}{h}\right) \tag{1}$$

where K is the constant of the structural forces and h is the characteristic length of the structural forces. The hydration repulsion energy per unit surface area between two parallel flat surfaces can be transformed to force terms by differentiating Eq. (1) with respect to separation distance z to yield

$$E_{\mathrm{H}}^{\mathrm{ff}} = K \exp\left(\frac{-z}{h}\right) \tag{2}$$

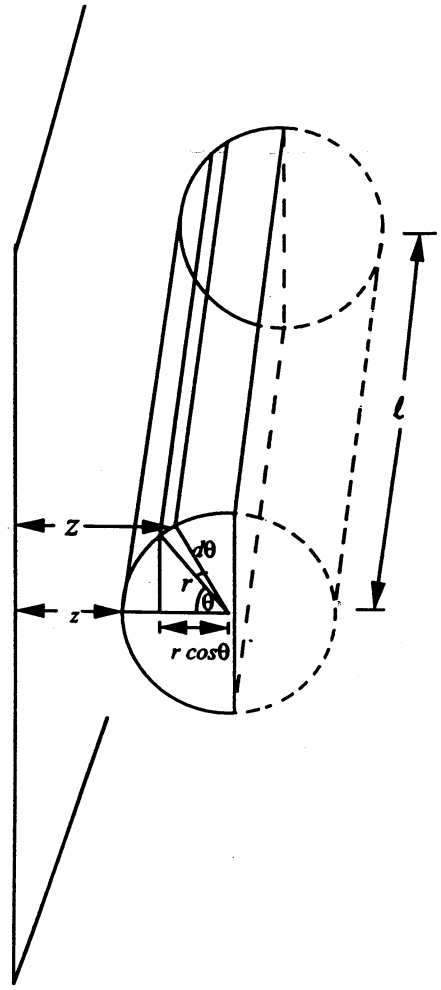

Fig. 2. Geometry of a flat plate–cylinder interaction.

2.1.2. Edge–face hydration force

The edge-face interaction has been modeled as the interaction between a flat plate and a half cylinder parallel to it as shown in Fig. 2. Interaction energy between a flat plate and a half cylinder of radius, r, is determined using Derjaguin's integration procedure [9]. In this method, the surface of the cylinder is thought to be divided into 'ribbons' of length, l, and width, $r\mathrm{d}\theta$ where l is the length and r is radius of the cylinder, and the angle θ has been shown in Fig. 2. If the radius of the cylinder is much larger than the separation distance, z, then the total interaction energy between the two surfaces could be found by integration of a series of separate interactions between the flat plate and the individual strips of width $r\mathrm{d}\theta$. The area of a small 'ribbon' $\mathrm{d}A$ is given by

$$dA = lr\ d\theta \tag{3}$$

If the distance of closest approach between the cylinder and the plate is given by z, then the variable distance Z between a small strip and the plate surface as a function of angle θ is given by

$$Z = z + r - r\cos\theta \tag{4}$$

Eqs. (1), (3) and (4) can be obtained to get the hydration energy (dE_H) between a small strip of area dA and the flat plate as given by

$$dE_H = kh\exp\left\{\frac{-(z + r - r\cos\theta)}{h}\right\} lr\ d\theta \tag{5}$$

The total interaction energy is the sum of interactions of all small strips of area dA with the flat surface.

$$E_H^{ef} = 2Khlr\exp\left(\frac{-z}{h}\right)\int_0^{\pi/2}\exp\left\{\frac{-r}{h}(1-\cos\theta)\right\} \times d\theta \tag{6}$$

Eq. (6) is multiplied by a factor of 2 in order to account for the interaction energy from the lower half of the cylinder (i.e. $-\pi/2 \le \theta \le 0$).

When the radius, r, is large compared with the separation distance, the hydration energy decreases rapidly with an increase in θ. Under these circumstances, [10] proposed the following approximate expression

$$\cos\theta = 1 - \frac{\theta^2}{2} \tag{7}$$

The error caused by the use of this expression in the case of electrostatic interaction between two parallel cylinders was found to be less than 1% for $\kappa r \ge 2.5$, where κ is Debye–Huckel parameter [11]. The error in the hydration energy expressions is expected to be even smaller than that because of the short-range nature of the hydration force. On substitution,

$$E_H^{ef} = 2Khlr\exp\left(\frac{-z}{h}\right)\int_0^{\pi/2}\exp\left(\frac{-r\theta^2}{2h}\right)d\theta \tag{8}$$

and integration of Eq. (8),

$$E_H^{ef} = 2Khlr\sqrt{\frac{2\pi h}{r}}\exp\left(\frac{-z}{h}\right)\left\{\Phi\left(\frac{\pi}{2}\sqrt{\frac{r}{h}}\right) - \Phi(0)\right\} \tag{9}$$

where $\Phi(x)$ is the error function, $\mathrm{erf}(x)$.

With typical dimensions of kaolinite, the radius of the kaolinite edge is taken as 82 nm, and the maximum value of h is around 2 nm for divalent ions as reported in the literature so that the value of $\pi/2\sqrt{r/h}$ is found to be 10. The function $\Phi(\pi/2\sqrt{r/h})$ approaches unity for the values of $\pi/2\sqrt{r/h}$ greater than around 4. Therefore, with an error of less than 0.003%, Eq. (9) simplifies to

$$E_H^{ef} = \sqrt{2}Khl\sqrt{\pi hr}\exp\left(\frac{-z}{h}\right) \tag{10}$$

The interaction in force terms is then given by

$$F_H^{ef} = \sqrt{2}Kl\sqrt{\pi hr}\exp\left(\frac{-z}{h}\right) \tag{11}$$

2.1.3. Edge–edge hydration force

The E–E interaction of kaolinite platelets is represented by the interaction between two parallel cylinders of equal radii. If the distance of closest approach between the two parallel cylinders is given by z, then the variable distance Z between the cylinders as a function of angle θ is given by

$$Z = z + 2r(1-\cos\theta) \tag{12}$$

Combining Eqs. (1), (3) and (12), and using the procedure described in the previous section, the hydration force between two interacting edges of the kaolinite platelets is obtained as

$$F_H^{ee} = Kl\sqrt{\pi hr}\exp\left(\frac{-z}{h}\right) \tag{13}$$

2.2. Born repulsion

2.2.1. Face–face Born repulsion force

A realistic formulation for Born repulsion, at least at the approximation level of the DLVO theory, would be the Hamaker-type integration of all molecules in the system [12]. Using this approach [13] developed a formula for sphere-plate Born repulsion

$$E_B = \frac{A\sigma^6}{7560}\left[\frac{8r+z}{(2r+z)^7} + \frac{6r-z}{z^7}\right] \tag{14}$$

in which the collision diameter σ is treated as a second characteristic property of the solids and

typically has a value of the order of 0.5 nm. For $r \gg z$, the Born repulsion in force terms between a sphere and a flat plate can be determined by differentiating Eq. (14) with respect to separation distance to give

$$F_B = \frac{Ar\sigma^6}{180z^8} \tag{15}$$

[9] expressed the force $F(z)$ between a sphere and a flat plate, which are distance z apart at their closest approach, in terms of energy per unit surface area between two flat parallel plates $E(z)$ which also are a distance z apart.

$$F(z)_{\text{Sphere-Plate}} = 2\pi r E(z)_{\text{Plate-Plate}} \tag{16}$$

In fact, Eq. (16) is valid for any type of force law, whether attractive, repulsive or oscillatory so long as the range of interaction and separation distances are much smaller than the radius of the sphere [2] or cylinder. Eqs. (15) and (16) give the Born repulsion energy between two flat plates as

$$E_B^{ff} = \frac{A\sigma^6}{360\pi z^8} \tag{17}$$

By differentiation, the Born repulsive force between two parallel flat plates is then given by

$$F_B^{ff} = \frac{A\sigma^6}{45\pi z^9} \tag{18}$$

2.2.2. Edge–face Born repulsion force

The following expression is obtained for the interactive force between an edge and a face surface using Eq. (17) and following the procedure adopted in the previous section.

$$F_B^{ef} = \frac{A\sigma^6 lr}{22.5\pi} \sum_{n=0}^{N} \frac{\Delta\theta}{\{z + r - r\cos(n\Delta\theta)\}^9} \tag{19}$$

Eq. (19) is found to be convergent within 5% of the final value for N equal to 550. The Born repulsion force for an E–F association could, therefore, be evaluated precisely using a simple computer code for larger values of N.

2.2.3. Edge–edge born repulsion force

The Born repulsive force between two interacting edges of kaolinite platelets is obtained using Eqs. (3), (12) and (17) as

$$F_B^{ee} = \frac{A\sigma^6 lr}{22.5\pi} \sum_{n=0}^{N} \frac{\Delta\theta}{\{z + 2r - 2r\cos(n\Delta\theta)\}^9} \tag{20}$$

Again, Eq. (20) is convergent for large values of N, and the Born repulsion could be estimated conveniently using a simple computer code.

2.3. Electrical double layer force

2.3.1. Face–face electrical double layer force

Using the Linear Superposition Approximation (LSA), [14] reported the following expression for the electrical double layer repulsion energy between two flat plates at potentials ψ_1 and ψ_2,

$$E_E^{LSA} = 32\varepsilon\kappa\left(\frac{kT}{ev}\right)^2 \tanh\left(\frac{ev\psi_1}{4kT}\right)\tanh\left(\frac{ev\psi_2}{4kT}\right) \times \exp(-\kappa z) \tag{21}$$

where ε is the permittivity of the medium; k, the Boltzmann constant; v, the valence of an ion; κ, the Debye–Hukel parameter; and T, the absolute temperature. For two parallel plates with the same potential (i.e. $\psi_1 = \psi_2$) the electrical double layer interaction in force terms is given by [14] as

$$F_E^{ff} = 32\varepsilon\kappa^2\left(\frac{kT}{ev}\right)^2\left\{\tanh\left(\frac{ev\psi_1}{4kT}\right)^2\right\}\exp(-\kappa z) \tag{22}$$

2.3.2. Edge–face electrical double layer force

Using the principle of LSA and Derjaguin's integration procedure, the interactive force between a flat plate and a cylinder of radius r is given by,

$$F_E^{ef} = 32\sqrt{2}\varepsilon l\kappa\sqrt{\pi\kappa r}\left(\frac{kT}{ev}\right)^2 \tanh\left(\frac{ev\psi_1}{4kT}\right)\tanh\left(\frac{ev\psi_2}{4kT}\right) \times \exp(-\kappa z) \tag{23}$$

2.3.3. Edge–edge electrical double layer force

Combining Eqs. (3), (12) and (21) and using Derjaguin's integration procedure gives the following final expression for the interaction between edges of two kaolinite platelets.

$$F_E^{ee} = 32\varepsilon l\kappa\sqrt{\pi\kappa r}\left(\frac{kT}{ev}\right)^2\left[\tanh\left(\frac{ev\psi_2}{4kT}\right)\right]^2\exp(-\kappa z) \tag{24}$$

2.4. van der Waals forces

2.4.1. Face–face van der Waals force

On the basis of Hamaker's approach [15], the attractive energy between two particles may be calculated by integration of the attractive energies from all atomic pairs formed by two atoms belonging to different particles. Based on the Hamaker method the potential energy of attraction per unit area between two flat plates of thickness, δ, is given by [10] as

$$E_V = \frac{-A}{12\pi}\left\{\frac{1}{z^2} + \frac{1}{(z+2\delta)^2} - \frac{1}{(z+\delta)^2}\right\} \tag{25}$$

where z is the distance of closest approach between two flat plates and A is the Hamaker constant. Since the thickness of the kaolinite platelets is much larger than the equilibrium separation distance between them, the last two terms of Eq. (25) can be neglected. The force of attraction in an F–F orientation is, therefore, given by

$$F_V^{ff} = -\frac{A}{6\pi z^3} \tag{26}$$

2.4.2. Edge–face van der Waals force

Using Hamaker's summation method, [2] developed an expression for the non-retarded van der Waals interaction energy between two parallel cylinders of radii r_1, and r_2, and length l, which is given by,

$$E_V^l = -\frac{Al}{12\sqrt{2}z^{3/2}}\left(\frac{r_1 r_2}{r_1 + r_2}\right)^{1/2} \tag{27}$$

The interaction between a cylinder and a flat plate is a special case of the interaction between two parallel cylinders, and it could be obtained in force terms by setting $r_1 \gg r_2$, and equal to r in Eq. (27) and differentiating it with respect to separation distance, z.

$$F_V^{ef} = -\frac{A}{8\sqrt{2}}\left(\frac{l}{r^2}\right)\left(\frac{r}{z}\right)^{5/2} \tag{28}$$

2.4.3. Edge–edge van der Waals force

The following expression is obtained in force terms for E–E interaction by setting $r_1 = r_2 = r$ and differentiating Eq. (27).

$$F_V^{ee} = -\frac{Al}{16r^2}\left(\frac{r}{z}\right)^{5/2} \tag{29}$$

It is important to note that the expressions for the hydration forces, electrical double layer forces (except F–F interactive force), and Born repulsion are original derivations made in this study, while expressions for van der Waals forces are given by others [2,11]. However, the ratios of E–F to E–E interactive forces among all four forces considered in this study remained constant with a multiplying factor of $\sqrt{2}$ for all the expressions developed in this work as well as the ones reported by others on van der Waals forces. This consistency also provides an indirect verification of the expressions derived in this work.

3. Experimental investigation

3.1. Materials

A sample of kaolinite clay provided by Dry Branch Kaolin Company, Georgia, was used in this study. The purity of the sample was checked by X-ray diffraction analysis, which showed two dominant peaks (3.58 and 7 Å), characterizing the sample as pure kaolinite with a moderate crystallinity [16]. A portion of the clay was dispersed in distilled water and the particle size analysis was performed using a Brinkmann particle size analyzer. The Brinkmann 2010 employs the time of transition theory, according to which the time it takes a laser beam moving at a fixed velocity to interact with a particle and cause a shadow on the detector is directly related to the particle diameter. The time period for which the scanning laser beam is blocked by a particle is multiplied by the scanning velocity in order to determine the particle size. The results of size analysis displayed the polydisperse nature of the sample with a mean size of 1.64 μm and standard deviation (S.D.) of 1.15 μm. Solid spherical particles made of soda-lime silica glass, supplied by Potters Industries Inc., were used as media grains for particle attachment. More than 90% of the particles were true spheres having a size range of 0.43–0.6 mm and a nominal size of 0.5 mm. Prior to their use, the glass beads were cleaned of adsorbed materials

using a procedure described by [17], which involved rinsing 700 cc glass beads with distilled water in a 1-l beaker and then sonication in 0.01-M NaOH for 10 min. The glass beads were then rinsed five times with distilled water followed by sonication in distilled water and 1-M HNO_3 for 10 min each. Finally, the glass beads were rinsed ten times with distilled water and the specific conductivity of the supernatant was checked. Rinsing with distilled water was stopped when the specific conductivity of the supernatant approached that of the distilled water used. Excess rinse water was drained and the beads were dried overnight in an oven at a constant temperature of 80°C.

3.2. Experimental procedure

Detachment experiments were done in two steps, an attachment step followed by a detachment step. Particle attachment was accomplished by preparing a kaolinite suspension using 6 l of filtered (through a 0.45-μm membrane filter) distilled water. Ionic strength and pH of the distilled water were adjusted using sodium chloride and 200 mg of precisely measured kaolinite was added. The resulting suspension was then stirred overnight. In order to maintain a constant pH throughout the attachment step, the pre-cleaned glass beads were also equilibrated overnight with a solution of the same chemical composition as that of the influent kaolinite suspension. The next day, all experimental apparatus was thoroughly cleaned using distilled water and a glass column of 27-mm diameter was packed with 175 g of equilibrated glass beads. Two liters of electrolyte having the same composition as that of the influent suspension (without particles) was prepared and filtered through 0.45-μm membrane filters. The filtered electrolyte was used to wash the freshly packed media with fluidization of the bed with an expansion of around 40%. This washing step prior to the start of particle attachment ensured the removal of contaminating particles from the system. Turbidity levels of less than 0.02 NTU were achieved at the end of fluidized washing. The packed column was tapped thoroughly until no further settlement was observed and a fixed bed height of around 0.2 m was achieved.

The kaolinite suspension was then filtered through the column in a once-through downflow mode of operation at the rate of 20 ml min^{-1} for 4 h. Stability of influent and effluent pH was ensured throughout the course of filtration and backwashing by frequent pH measurements. During filtration, all effluent was collected for later mass measurements. Immediately after the particle attachment was completed, the column was backwashed under fluidized conditions with a 20% bed expansion, which corresponded to a flow rate of 170 ml min^{-1} and a velocity of 0.495 cm s^{-1}. Particle detachment was completed in 19 min and all backwash water (3.2 l) was collected for subsequent mass measurements. The kinetics of particle detachment varied from being very high in the beginning to very low at the end of backwashing. The total detachment of particles was studied in these experiments. The backwash water, filter effluent, and the leftover portion of the influent suspension were filtered through glass fiber filters for kaolinite mass measurements. In each case, the turbidity of the filtrate was found to be at background levels, which ensured almost complete capture of the clay platelets on the filter papers. The percent detachment (as mass) was then determined by mass balances.

4. Results and discussion

Depending upon the chemistry of the suspending medium, kaolinite platelets may flocculate in E–E, E–F, or F–F modes of interaction. Adsorbed organic coatings have also been reported to influence the predominant mode of interaction [18]. Variations in the modes of association in response to changes in the chemistry of the suspending medium may determine the nature of the resulting deposits during particle attachment. It has been hypothesized that the detachment of particles of deposited in a porous media may be affected by the nature of the deposit undergoing erosion [19]. A knowledge of the dominant modes of interaction of kaolinite platelets as a function of solution pH would, therefore, be helpful in mechanistic understanding of the phenomenon of detachment of asymmetric particles.

Theoretical expressions for the F–F, E–F and E–E modes of association in kaolinite platelets, which were developed in the previous section, have been used to explain the experimental results semi-quantitatively. In the theoretical force calculations, a value of 2.6×10^{-20} J, as measured by [20] for kaolinite, has been used for Hamaker constant, whereas Born repulsion is estimated using a collision diameter of 0.5 nm, which is a typical value and has frequently been used in the literature [13,3]. Born repulsion is very short range in nature and it decays so steeply with distance, that some researchers consider it to be most reasonable to depict Born repulsion in total interaction energy plots as a vertical straight line, located around 0.136 nm from the origin [21]. A sensitivity analysis showed that significant effects of variations in the value of collision diameter could only be seen at distances of separation much less than 1 nm. The value of the collision diameter was found to change the location of primary minima only slightly and did not affect the rest of the total force curves significantly. In quantification of the hydration force, a characteristic decay length of 0.9 nm has been used in conjunction with a value of 1.6×10^6 N m^{-2} for the hydration force constant. The force constants have been selected from the literature-reported values, a summary of which has been presented in [22]. The adopted value of 0.9 nm for the characteristic decay length lies well within the already narrow range (0.85–1 nm) of literature-reported values. The adopted value of 1.6×10^6 N m^{-2} for the hydration force constant matches well with the values 1.5×10^6 and 2×10^6 N m^{-2} reported for glass and montmorillonite, respectively [23,24]. In fact, selection of all force constants was based on sensitivity analysis for the force constants performed by [25]. In the quantification of electrical double layer forces, zeta potential values for the edge and face of a platelet, as a function of pH and ionic strength, measured by [26,27,6] were adopted.

The 'Total interactive force', that is plotted on the *Y*-axis of the Figs. 3–6, represents the sum of all four forces considered in this study. Fig. 3 shows the total interactive force in nanoNewtons (nN) between kaolinite platelets held in F–F, E–F, and E–E modes of association as a function of separation distance at pH 3. The two approaching clay platelets will only attach in the E–E mode of association if they surmount the repulsive force barrier and fall into the primary force minimum. At the primary force minimum, the attractive forces balance the repulsive forces and the platelets remain in equilibrium. Any unbalance in the equilibrium of the microscopic forces in favor of particle pull-off, as caused by hydrodynamic and/or chemical and colloidal forces, may lead to detachment of the platelets.

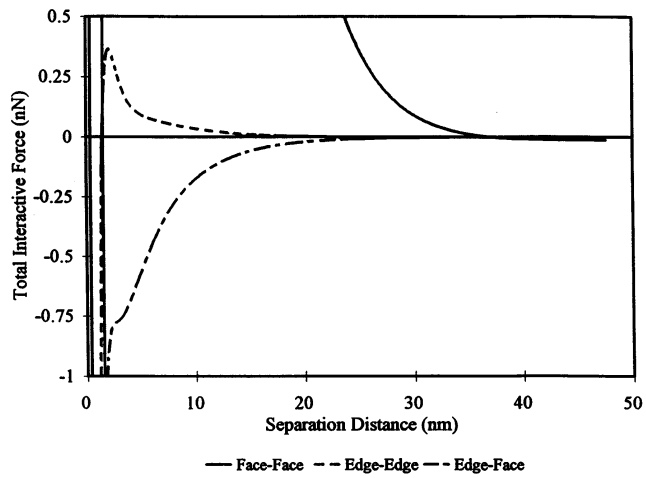

Fig. 3. Total interactive force between kaolinite platelets as predicted by the model at pH 3 (IS = 0.004 M; edge charge = + 22 mV, face charge = − 42 mV).

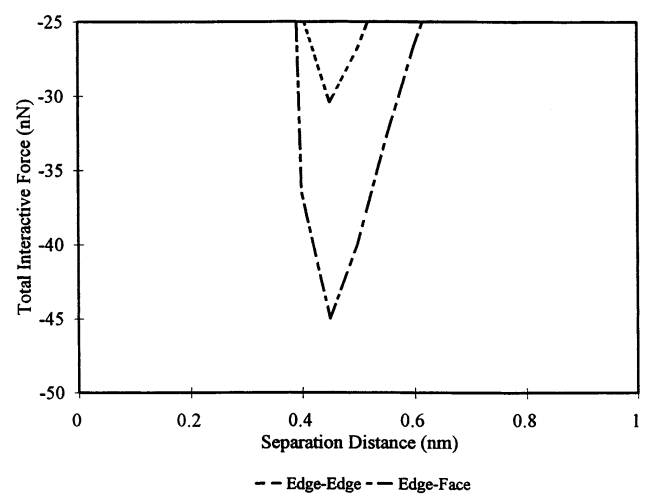

Fig. 4. Adhesive forces for E–F and E–E modes of interaction as predicted by the model at pH 3 (IS = 0.004 M; edge charge = + 22 mV; face charge = − 42 mV).

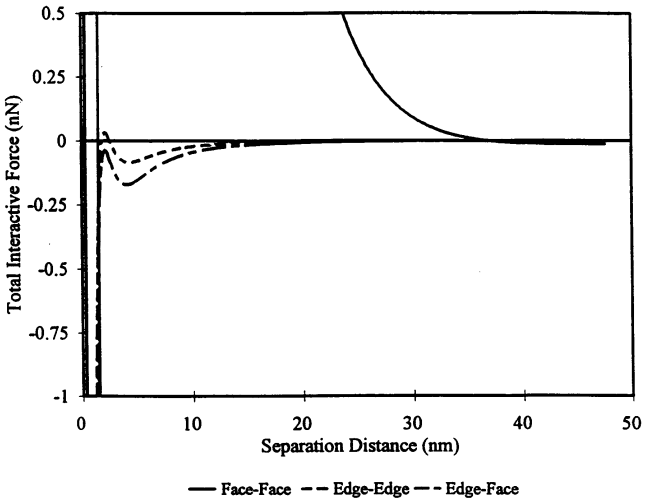

Fig. 5. Total interactive force between kaolinite platelets as predicted by the model at pH 7 (IS = 0.004 M; edge charge = + 2 mV, face charge = − 42 mV).

Force calculations show that all three modes of interaction have finite depths of primary minima. The depth of the primary minimum is the least (30 nN) for an E–E mode of interaction, whereas a relatively deeper primary minimum (45 Nan) is observed in the case of an E–F interaction as depicted by Fig. 4. At the same pH and ionic strength, the F–F interaction displayed a very deep primary minimum of around 12 000 nN (not shown in Fig. 4). The depth of the primary minima, and therefore, the magnitude of the adhesive force follows the sequence FF ≫ EF > EE. In an F–F interaction, a very deep primary minimum indicates a very strong association, but a large force barrier that extends to a separation distance of around 35 nm (Fig. 3) limits interparticle approach and hence attachment. At this pH, a relatively small fraction of the particles colliding in an F–F mode could, therefore, be expected to surmount this barrier. The E–E mode of interaction in Fig. 3 also shows a repulsive force barrier at close approach that extends up to a separation distance of around 15 nm and makes this mode of association less likely too. The E–F orientation shows an attractive force between the two platelets at all separation distances. The E–F attractive force becomes prominent at a considerably large separation distance of greater than 20 nm and then continues to increase monotonically until the equilibrium separation distance (primary force minimum) is reached. Force calculations presented in Fig. 3 suggest clearly that the most likely mode of association at pH 3 is E–F.

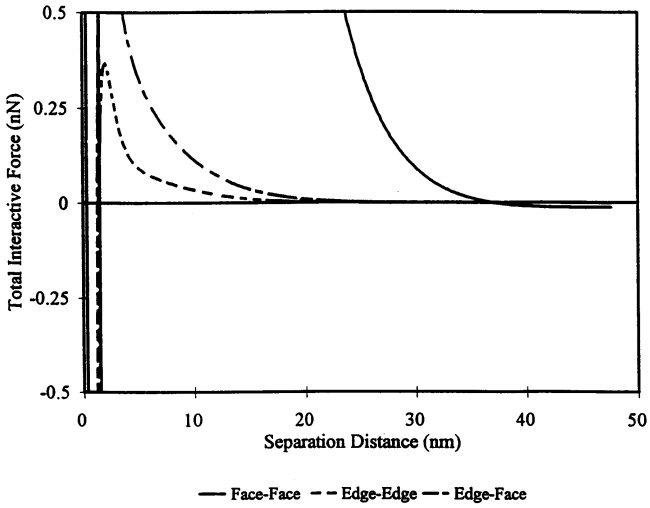

Fig. 6. Total interactive force between kaolinite platelets as predicted by the model at pH 9 (IS = 0.004 M; edge charge = − 22 mV; face charge = − 42 mV).

At pH 5, force calculations for the F–F interaction showed no change, which is consistent with the nature of charge on platelet faces. The origin of charge on platelet faces is isomorphous replacement, and there is no evidence for a pH dependent charge density at the basal surfaces of kaolinite particles [28]. Under these circumstances, an F–F interaction should be independent of solution pH. A repulsive force barrier in the case of an E–E mode of interaction was still evidenced at pH 5, although its height and extent had decreased. The E–F orientation showed and attractive force at all separation distances suggesting that E–F is also the preferred mode of interaction at pH 5.

At pH 7, which is close to the isoelectric point of the edge surface [26], both E–F and E–E interactions produced almost identical force curves as shown in Fig. 5, although the depth of the primary minimum (and therefore, the adhesive force) for an E–F interaction is still larger than that of an E–E interaction. Particle associations in both E–E and E–F modes of interaction are, therefore, likely to occur at this pH.

Total force calculations at pH 9 are presented in Fig. 6, where all three modes of interaction

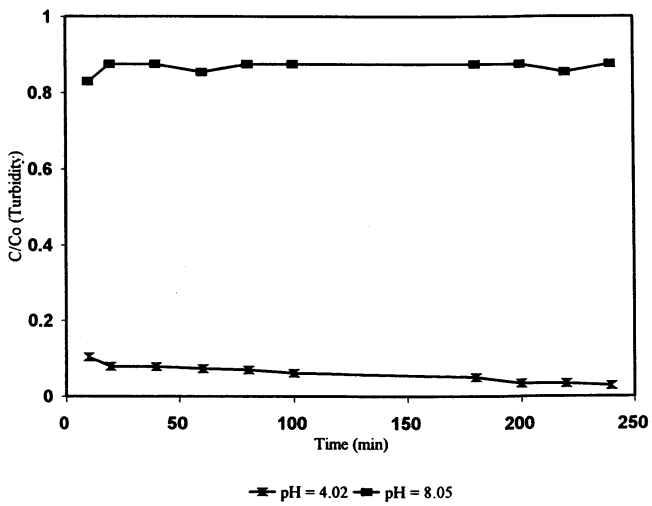

Fig. 7. Filtration of kaolinite at constant ionic strength.

display repulsive force barriers. The heights of the force barriers decrease in the order F–F > E–F > E–E. The repulsive force barriers present in all three modes of interaction will not only keep platelets from flocculation in any of the F–F, E–F, or E–E modes of interaction but also from attachment to other negatively charged surfaces. This hypothesis was validated experimentally by depositing kaolinite platelets in porous media columns. A sample of experimental results on kaolinite particle attachment at pH 4.02 and 8.05 is shown in Fig. 7, where C and Co represent effluent and influent suspension turbidities, respectively. The normalized filter effluent turbidity (C/Co) at pH 8.05 was found to be greater than 0.8 as compared with a value of less than 0.1 at pH 4.02, which demonstrates highly dispersive characteristics of the kaolinite platelets at pH 8.05. Also, in rheological studies of aqueous clay suspensions [28] found kaolinite platelets to be very dispersed at pH above around 8.

F–F associations are expected to be independent of solution pH since the negative charge on the basal planes of the kaolinite platelets originates due to isomorphous substitutions. The extent of F–F associations may, therefore, be the same at all pH values under constant ionic strength conditions. The edge charge, on the other hand, originates as a result of broken bonds at the edges and it is a function of pH. Therefore, the extent of E–F and E–E associations should essentially be dependent on pH. At low value of pH, the E–F interactions are highly favorable (Fig. 3); however, platelets approaching in E–E and F–F orientations may also cause flocculation if the driving force is sufficiently large to surmount the repulsive force barrier. The relative abundance of F–F interactions may be small at low values of pH because the total number of E–F associations is very large. An increase in pH affects both E–F and E–E associations adversely while keeping the colloidal forces unaltered for the F–F associations (Figs. 3, 5 and 6). It is, therefore, expected that the relative abundance of F–F associations increases gradually as the pH is increased.

It is important to note that the quantification, and therefore comparison, of net adhesive forces among the three modes of interaction was made possible only after inclusion of short range effects into DLVO theory. The extended DLVO theory presented in this publication predicts finite depths and locations of primary minima, as shown in Fig. 4, in contrast to unrealistic infinitely deep primary minima obtained by others [4,6,29] considering DLVO interaction energies alone. This obviates the necessity for assuming a separation distance as in DLVO theory alone.

The results of detachment experiments are shown in Fig. 8. The release of kaolinite platelets was found to be dependent on pH of the influent suspension during attachment, and a maximum in

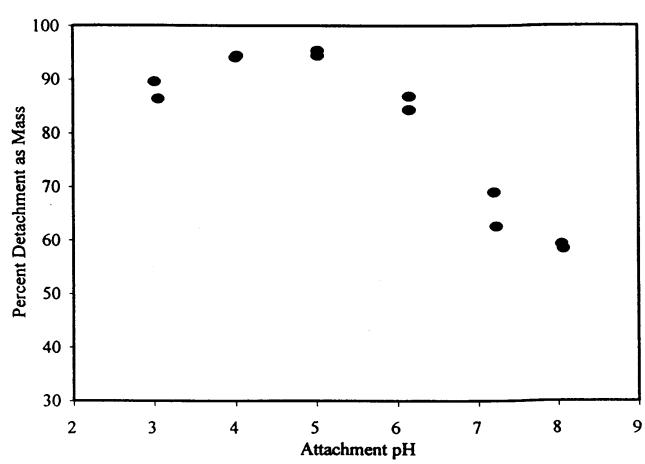

Fig. 8. Effect of attachment pH on detachment of kaolinite platelets.

percent mass detachment was observed at a pH value around 5. A similar trend of kaolinite erosion from a bed simulating a stream was observed in a subsequent study using a tilting flume under uniform flow conditions [30]. The observed behavior of kaolinite detachment can be explained using the theoretical micromechanics model developed in this study. The most likely association at pH 3 is E–F, where the electrostatic attraction in conjunction with van der Waals forces creates relatively stronger and longer range attraction between an edge and a face of two interacting platelets. It is worthwhile to emphasize that when the two surfaces are oppositely charged, the electrical forces become attractive, and instead of countering the van der Waals forces (as they do in the case of similarly charged surfaces), they reinforce them instead of giving rise to a long-range, strong net attraction. Force calculations show that in the case of E–F interactions, the depth of the primary minima decreases with an increase in pH. Therefore, as the pH is raised above 3, the adhesive forces holding the clay platelets in an E–F mode of interaction become weaker, which allows particle release to occur more easily and causes percent detachment to increase as observed in Fig. 8. An E–F association is inherently stronger than an E–E association by a factor of $\sqrt{2}$, which is evident from the expressions developed for the hydration forces, electrical double layer forces, Born repulsion, and van der Waals forces. Total force calculations show that the depth of the primary minimum for an E–E orientation is 31 nN as compared with a depth of 44 nN in the case of an E–F association at pH 5. The greater depth of primary minimum for an E–F interaction than that of an E–E association suggests that the particles which attach in an E–E orientation could be detached more easily as compared with those attached in an E–F mode. The force calculations also reveal that as the pH is increased from 3, the fraction of attached platelets held in an E–E mode of association increases. This gradual increase in contributions of the week E–E associations contributes further to the increase in percent detachment up to pH around 5 as shown in Fig. 8.

At higher values of pH (above 7), the relative contribution of F–F associations to the total interparticle associations may be expected to increase. The predominance of F–F structures at higher pH values has also been suggested in the literature. Based on the dense and compact nature of settled kaolinite deposits in conjunction with their low water content, [31] suggested that the associations at high pH (>7) are predominantly F–F. As shown by the force calculations, F–F associations, F–F associations are very strong and give rise to card-pack structures. Particles held in this mode of association will resist the eroding forces much more than those held by other modes of association. The observed decrease in percent mass detachment at high pH values in Fig. 8 could, therefore, be attributed to the increased fraction of F–F associations. Also, the F–F associations give rise to dense, tightly packed flake-like structures [28,32], whereas E–E and E–F interactions result in voluminous, three-dimensional, cardhouse-like structures of high void ratio [32]. It is hypothesized that the dense, flake-like structures attached to a surface will protrude less into the fluid boundary layer as compared with voluminous, cardhouse-like structures. Under conditions of constants fluid shear stress, the compact F–F structures may experience relatively smaller hydrodynamic forces than those experienced by the cardhouse-like voluminous E–E and E–F structures and hence will detach less as shown in Fig. 8.

5. Conclusions

It is realistic and reasonable to analyze interactions between kaolinite particles considering their actual platelet-like shape instead of making use of oversimplifying assumptions of particle sphericity. The microscopic force model developed on the basis of hexagonal platelet-like shape of kaolinite particles was found to be consistent with experimental observations on attachment and detachment of kaolinite particles.

The microscopic force analysis showed that the total interactive force between the two interacting particles varies drastically with their geometric

shape. Under constant chemical conditions, the three geometric modes of interaction (E–E, E–F, and F–F) of the kaolinite platelets showed significantly different total force curves. The depth of the primary minima and, therefore, the magnitude of the adhesive force followed the sequence F–F > E–F > E–E. The expressions developed for the E–F mode of interaction for hydration forces, Born repulsion, electrical double layer forces, and van der Waals forces showed stronger interactive forces than those for E–E mode of association by a factor of $\sqrt{2}$.

The release of kaolinite platelets under constant chemical conditions during particle detachment was found to be dependent on the pH of the suspension used during particle attachment. Kaolinite platelets showed a maximum in the percent detachment at an attachment pH around 5. The variations in the interparticle adhesive forces, both within a specific mode of interaction and due to changes in the predominant modes of interaction with pH, were found to explain the maximum percent detachment observed experimentally at a pH value around 5.

Acknowledgements

This research was funded by the USEPA Hazardous Substance Research Center, South and Southwest and was conducted at the School of Civil and Environmental Engineering of the Georgia Institute of Technology.

References

[1] R.J. Hunter, Introduction to Modern Colloid Science, Oxford Science Publications, Oxford, 1993.
[2] J.N. Israelachvili, Intermolecular and Surface Forces, second ed., Academic Press, New York, 1991.
[3] P. Raveendran, A. Amirtharajah, J. Environ. Eng. ASCE 121 (1995) 860.
[4] A.W. Flegmann, J.W. Goodwin, R.H. Ottewill, Proc. Br. Ceram. Soc. 13 (1969) 31.
[5] C.E. Weaver, Clays Clay Miner. 24 (1976) 215.
[6] A.E. James, D.J. Williams, Adv. Colloid Interf. Sci. 17 (1982) 219.
[7] A. Amirtharajah, J. Environ. Eng. Div. ASCE 104 (1978) 917.
[8] N.V. Churaev, B.V. Derjaguin, J. Colloid Interf. Sci. 103 (1985) 542.
[9] B.V. Derjaguin, Kolloid Z. 69 (1934) 115.
[10] E.J.W. Verwey, J.T.G. Overbeek, Theory of the Stability of Lyophobic Colloids, Elsevier, Amsterdam, 1948.
[11] M.J. Sparnaay, Recueil des Travaux Chimiques des Pays-Bas 78 (1959) 680.
[12] M. Elimelech, J. Gregory, X. Jia, R.A Williams, Particle Deposition and Aggregation: Measurement, Modeling, and Simulation, Butterworth Heinemann, London, UK, 1995.
[13] E. Ruckenstein, D.C. Prieve, Am. Inst. Chem. Eng. J. 22 (1976) 276.
[14] J. Gregory, J. Colloid Interf. Sci. 51 (1975) 44.
[15] H.C. Hamaker, Physica 4 (1937) 1058.
[16] C.E. Weaver, Personal Communications, Georgia Institute of Technology, Atlanta, GA, USA, 1994.
[17] J.E. Tobiason, Ph.D. dissertation, The Johns Hopkins University, Baltimore, MD, USA, 1987.
[18] K.E. Dennett, T.W. Sturm, A. Amirtharajah, T. Mahmood, Water Environ. Res. 70 (1998) 268.
[19] T. Mahmood, A. Amirtharajah, T.W. Sturm, K.E. Dennett, Proceedings of 1995 ASCE National Conference, Georgia, USA, 1995 p. 47.
[20] J.T. Welzen, H.N. Stein, J.M. Stevens, C.A. Sisken, J. Colloid Interf. Sci. 81 (1981) 455.
[21] C.J. Van Oss, Interfacial Forces in Aqueous Media, Marcel Dekker, New York, 1994.
[22] T. Mahmood, 1996, Ph.D. dissertation, Georgia Institute of Technology, Atlanta, GA, USA.
[23] Y.I. Rabinovich, B.V. Derjaguin, N.V. Churaev, Adv. Colloid Interf. Sci. 16 (1982) 63.
[24] J.L. Oliphant, P.P. Low, J. Colloid Interf. Sci. 89 (1982) 366.
[25] P. Raveendran, Ph.D. dissertation, Georgia Institute of Technology, Atlanta, GA, USA, 1993.
[26] D.J.A. Williams, K.P. Williams, Trans. J. Br. Ceram. Soc. 81 (1982) 78.
[27] D.J.A. Williams, K.P. Williams, J. Colloid Interf. Sci. 65 (1978) 79.
[28] B. Rand, I.E. Melton, J. Colloid Interf. Sci. 60 (1977) 308.
[29] R. Kuo, E. Matijevic, J. Chem. Soc. Faraday Trans. I. 75 (8) (1978) 2014.
[30] V. Ravisangar, M.S. thesis, Georgia Institute of Technology, Atlanta, GA, USA, 1996.
[31] K.E. Dennett, Ph.D. dissertation, Georgia Institute of Technology, Atlanta, GA, USA, 1995.
[32] H. van Olphen, An Introduction to Clay Colloid Chemistry for Clay Technologists, Geologists, and Soil Scientists, second ed., Wiley, New York, 1977.